Time-Domain Investigation of Electron Recapture via Post-Collision Interaction in a Double Photoionization Continuum

S. N. Pisharody and R. R. Jones

Department of Physics, University of Virginia, Charlottesville, Virginia 22904-4714, USA

(Received 17 June 2003; published 11 November 2003)

Picosecond laser pulses have been used to sequentially photoionize both valence electrons from neutral Ba atoms, producing two radially localized continuum wave packets. The Coulomb interaction between the two outgoing electrons can result in the recapture of one of the electrons by the parent ion. The energy distribution of Rydberg ions formed via this ''post-collision'' interaction is measured as a function of the delay between the ionizing laser pulses. The experimental data are in agreement with the results of both a quantum sudden approximation and a classical simulation.

DOI: 10.1103/PhysRevLett.91.203002 PACS numbers: 32.80.Fb, 32.80.Qk, 32.80.Rm

The dynamical evolution of charged particles in a three-body Coulomb continuum remains a fundamental unsolved problem in quantum mechanics [1]. Because of the long-range Coulomb interaction between the charges, the continuum eigenstates are highly correlated, having little resemblance to those of three, independent free particles. In the time domain, the motion of each particle depends critically on that of the others, and is characterized by time-dependent energy and angular momentum exchange between charges. Post-collision interaction (PCI) is a generic label that has been given to this multiparticle coupling. The importance of PCI in ionizing collisions (ions or electrons incident on neutral atoms) or photoionization (direct double photoionization or single ionization followed by Auger) is well documented [2–7].

The effect of PCI on the energy and/or angular distributions of charged particles has been explored as a function of incident ion, electron, or photon energy [2,5,7]. Such measurements test the accuracy of approximate methods for computing multi-particle eigenstate compositions at particular final-state energies [1,3–7]. Yet in spite of the fact that measurements are performed in the frequency domain, intuitive semiclassical pictures of time-dependent charge screening or particle scattering are often used to describe experiments or motivate theoretical approaches to these problems [3–5]. To the best of our knowledge, the experiments described here are actually the first to explore PCI directly in the time domain.

Specifically, we consider electron capture facilitated by PCI following double ionization. In the experiment, picosecond laser pulses sequentially ionize the two 6*s* valence electrons in Ba. Initially, one electron e_1 is photoionized just above the $5d_{5/2}\epsilon d$ continuum threshold. As depicted in Fig. 1, e_1 moves in the Coulomb potential of the singly charged $5d$ Ba^+ ion and travels outward in the form of a radially localized continuum wave packet. After a short delay the $5d^+$ ion is photoionized, producing a second continuum electron e_2 with near zero total energy relative to the Ba^{2+} threshold. Because e_1 has moved far from the ion, its presence has negligible influence on the initial motion of e_2. Therefore, e_2 leaves the vicinity of the ion as a radially localized packet in a doubly charged Coulomb potential. As described in detail below, the ''inner'' wave packet expands more rapidly than the ''outer'' wave packet, e_2 overtakes e_1, and Coulomb repulsion facilitates energy and momentum exchange between the two electrons. Sufficient energy loss by one electron results in its capture into a Ba^+ Rydberg state [5]. Using selective field ionization [8], we find that the Rydberg ion yield and energy distribution depend critically on the delay τ between the two, precisely controlled, ionization events.

Ba atoms in a thermal beam are exposed to four laser pulses. First, a 5 ns, 350.2 nm dye laser pulse (L1) excites atoms in the $6s6s$ ground state to an intermediate $5d6p$ level (see Fig. 1). Immediately following L1, a 700 fs, 524 nm laser pulse (L2) photoionizes the $5d6p$ atoms, primarily into the $5d_{5/2}\epsilon dJ = 0$ continuum. L2 is produced in an optical parametric amplifier (OPA1) that is pumped by the second harmonic of a portion of the beam from an amplified 770 nm, 220 fs Ti:sapphire laser. The bandwidth of the Ti:sapphire laser and L2 are restricted to reduce dispersion in the outgoing wave packet which has

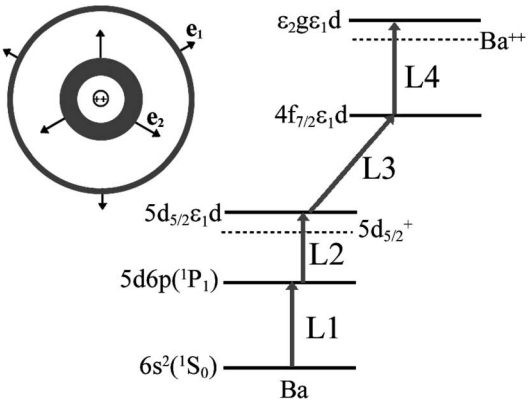

FIG. 1. Schematic laser excitation diagram and depiction of the initial expansion of two concentric radially localized continuum wave packets.

an energy bandwidth approximately equal to its mean energy, $E_{1i} \simeq 20\ \mathrm{cm}^{-1}$. After a delay τ, a 300 fs, 233 nm pulse (L3) excites the Ba^+ ion from the $5d_{5/2}$ level to an intermediate $4f_{7/2}$ state. L3 is created by mixing the 385 nm, 250 fs second harmonic of the Ti:sapphire laser with the 590 nm, 250 fs output of a second optical parametric amplifer (OPA2). A 500 fsec, 312 nm pulse (L4) is coincident in time with L3 and photoionizes the $4f_{7/2}$ ions just above the Ba^{2+} threshold. L4 is produced by mixing the 524 nm, 1 ps output of OPA1 with the 770 nm Ti:sapphire fundamental. The second outgoing wave packet e_2 also has an energy distribution whose width is approximately equal to its mean energy, $E_{2i} \simeq 30\ \mathrm{cm}^{-1}$. All four laser pulses are linearly polarized in the z direction, so the projection M of total angular momentum on this axis is zero.

Because a large number of ions are formed during the laser excitation, a two-stage time-of-flight spectrometer is employed to detect, nearly background free, any Rydberg ions formed by PCI. The lasers and atoms interact between two parallel conducting plates that are separated by 1 cm. Approximately 10 ns after L4, a 15 V "clearing" pulse is applied to the lower conductor and pushes any positive ions in the interaction region through a copper mesh covered, 0.5 cm diameter hole in the upper conductor, also known as the "extraction" plate. A grounded, copper mesh is positioned 0.7 cm above the extraction plate and defines a second, uniform electric field region. Ba^+ ions move into the second field just as a -4.5 kV field ionization pulse is applied to the extraction plate. Any singly charged Rydberg ions that are produced via PCI and have principal quantum numbers $115 > n > 28$ are not ionized by the clearing pulse but are ionized during the 500 ns rise of the field ionization pulse. Only those electrons that are liberated in the second field region are pushed into a microchannel plate detector.

The arrival time of each electron identifies the field at which it ionized and, therefore, its approximate principal quantum number. Because of the finite size of the laser excitation volume and the differences in the field ionization thresholds for states of the same n but different angular momentum quantum numbers ℓ and m, an electron's arrival time does not uniquely determine its binding energy prior to ionization. Consequently, the time-dependent field ionized electron signal appears as a single broad feature that is $\sim$100 ns long. Rydberg ions with a range of principal quantum numbers contribute to the signal in any given time interval. For analysis, we divide the signal into seven adjacent time bins. Each bin or "gate" is associated with the principal quantum number N which is the most probable contributor to the signal in that gate. The value of N and range of n states contributing to each bin are calibrated by replacing L4 with a tunable, 310–330 nm, 5 ns dye laser pulse (L5) which directly excites Ba^+ ng eigenstates from Ba^+ $4f_{7/2}$ ions. The electron arrival times are recorded as the frequency of L5 is scanned over the Ba^+ ng Rydberg series.

Figure 2 shows the field ionization signal in two different time bins as a function of the delay τ between the two pairs of laser pulses that photoionize e_1 and e_2, respectively. The probability for recapture into weakly bound states $N \simeq 69$ is plotted in Fig. 2(a), while Fig. 2(b) displays the population in more tightly bound levels, $N \simeq 49$. The delay-dependent signals in the other bins are qualitatively similar. The recapture probability is largest when the lasers overlap in time and falls steadily with increasing delay. Because of the finite duration of the laser pulses, the signal in all gates rises in $\simeq 1.5$ ps. However, the population in the more tightly bound levels peaks at slightly smaller delays than that of the high-n states. In addition, the recapture probability drops more sharply for lower-n states. These effects are also seen in Fig. 3 where the fractional population in each time bin is plotted for three different time delays.

The qualitative features in the data are readily understood by considering the time-dependent interaction between two expanding, radially localized, continuum wave packets. The Coulomb repulsion between electrons is conveniently expanded as

$$V_{ee} = \frac{1}{|\vec{r}_1 - \vec{r}_2|} = \sum_{k=0}^{\infty} \frac{r_<^k}{r_>^{k+1}} P_k(\cos\gamma), \qquad (1)$$

where $r_<$ ($r_>$) is the lesser (greater) of r_1 and r_2, γ is the angle between the position vectors of the two electrons $\vec{r}_1$ and $\vec{r}_2$, and P_k is a Legendre polynomial. Unless otherwise noted, atomic units are used throughout. Immediately following its photoionization, e_1 moves rapidly away from e_2 and the Ba^{2+} core such that $r_1 \gg r_2$. Under these initial conditions, only the $k = 0$ term in Eq. (1) is non-negligible, and the electron-electron interaction $V_{ee} \simeq \frac{1}{r_1}$ isotropically screens the Ba^{2+} potential. Assuming a pure doubly charged Coulomb potential for the Ba^{2+} core, the two-electron potential in this initial

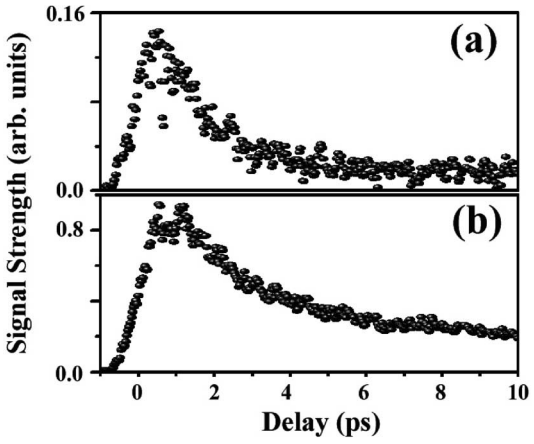

FIG. 2. Electron recapture signal in two different time bins as a function of delay between the launch of the two wave packets. In (a) and (b) ionic Rydberg electrons with the greatest contribution to the bin have $N \simeq 49$ and $N \simeq 69$, respectively.

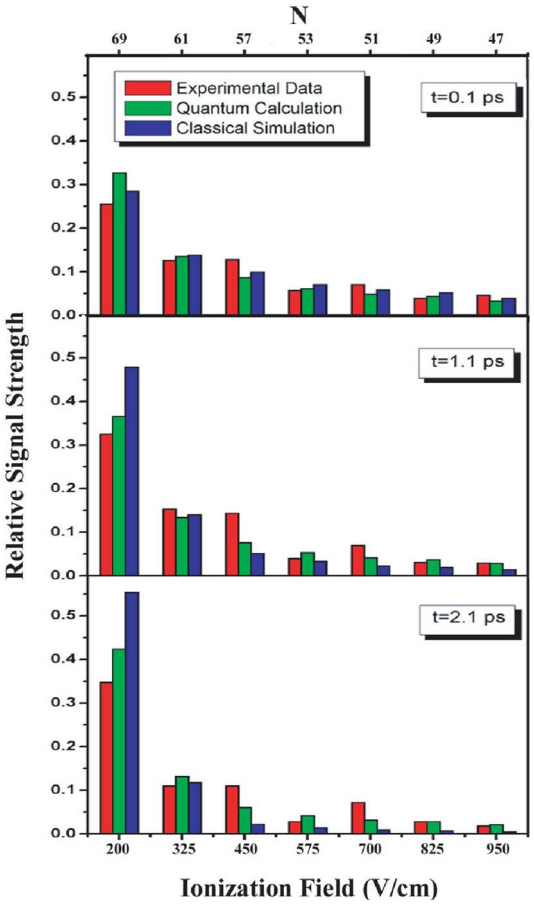

FIG. 3 (color online). Experimental and simulated relative recapture yields in different time bins for three different wave packet launch delays. The lower horizontal axis shows the ionizing field at which Rydberg electrons are liberated and the upper horizontal axis shows the ionic n state N that contributes most to the respective bins. The location of the quantum simulation data bar corresponds to the value of N determined for each bin.

configuration is separable $V_0(\vec{r}_1, \vec{r}_2) = \frac{-1}{r_1} + \frac{-2}{r_2}$, justifying our description of the initial state of the system in terms of two distinct electron wave packets.

After a delay τ, e_2 is launched as a second, outgoing radial wave packet. Initially both electrons have total energies, $E_{1i}, E_{2i} \approx 0$ in their respective isotropic potentials. If we continue to consider only the $k = 0$ term in V_{ee}, then the radial velocities of e_1 and e_2 are $v_1 \simeq \sqrt{2/r_1}$ and $v_2 \simeq \sqrt{4/r_2}$, respectively. Because of its higher radial velocity, e_2 overtakes e_1 at a distance $R = r_1 = r_2$ from nucleus. The "crossing" radius R is a monotonically increasing function of the delay between the launch of the two wave packets. The definition of outer and inner electron reverses instantly as wave packet e_2 passes through wave packet e_1. e_2 suddenly feels a singly charged potential while e_1 experiences the full charge of the Ba^{2+} ion. The total energy of e_2 increases to $E_{2f} = E_{2i} + 1/R$ and that of e_1 decreases to $E_{1f} = E_{1i} - 1/R$. Thus, e_2 remains in the continuum and continues to move away from the ion core, but if

$$E_{1f} = \frac{-2}{n^2} = E_{1i} - \frac{1}{R} < 0, \tag{2}$$

e_1 is recaptured and moves as a bound wave packet in the Ba^{2+} potential.

The zeroth-order recapture condition [Eq. (2)] predicts more tightly bound ionic wave packets for smaller crossing radii R, i.e., for shorter delays τ. Furthermore, the constituent eigenstates in the final ionic wave packet should have principal quantum numbers $n > \sqrt{2R}$. Hence, more lower-n Rydberg ions are produced at short delays and only higher-n states are created for larger values of τ. These predictions are in good qualitative agreement with the experimental data in Figs. 2 and 3.

The analysis can be made more quantitative by considering the effects of the sudden potential change on the continuum wave packet e_1 that is actually created in the experiment. We numerically construct a quasicontinuum radial wave packet, $\Psi(r_1, t) = \sum_k \psi_k(r_1) e^{-iE_k t}$ with mean energy $E_{1i} = 15\ \mathrm{cm}^{-1}$ and a $10\ \mathrm{cm}^{-1}$ FWHM Gaussian energy distribution, by superposing approximately 200, $\ell = 2, Z_1 = 1$ Coulomb continuum eigenfunctions, $\psi_k(r_1)$, that are separated in energy by $\delta E_k = 0.1\ \mathrm{cm}^{-1}$. The wave packet, which is localized near the origin at $t = 0$, propagates radially outward for $t > 0$. PCI due to the passing of e_2 is simulated by projecting $\Psi(r_1, t)$ onto the eigenstates of the $Z_1 = 2$ Coulomb potential. Population "shaken" into ionic bound states with $115 > n > 28$ represents the observable recapture signal at $t = \tau$ [9]. Using the experimentally determined electron time of arrival to n-state calibration, the simulated recapture yield is sorted into time bins that match those used in the experiment. The calculated relative signal strength in each bin is compared to the experimental data in Fig. 3. Considering the simplicity of the quantum sudden approximation, the agreement between experiment and simulation is quite good.

Of course, the sudden potential change or "shake" approximation has been used with considerable success in previous studies of PCI [3–5] and inner electron ionization [10]. Therefore, its effectiveness may not seem surprising. However, we note that previous investigations have been performed under conditions where the approximation is strictly valid, i.e., where a fast inner electron e_2 moves very rapidly through a much slower outer electron e_1. In that case, the two electrons are at comparable radii, $r_1 \sim r_2$, for only a very brief time, and the higher-order ($k > 0$) terms in V_{ee} have a negligible time-integrated effect on the electrons' energy and angular momentum.

The situation is considerably different in the current experiment. As noted above, the radial velocities of our two electrons differ by only ~40% at the crossing radius R. Consequently, in the absence of the higher-order interaction terms, the two wave packets overlap in space for ~1 ps, a time during which the wave packets can move a distance comparable to R. In this light, the good agreement between the data and the sudden approximation

results is surprising [11]. In particular, because angular coupling between the electrons occurs only through the higher-order terms in V_{ee}, the success of the shakeup model suggests that significant angular momentum exchange is not present [4]. Unfortunately, we know of no straightforward method for measuring the angular momentum of the recaptured Rydberg ions. Instead, we attempt to illuminate the precise role of the higher-order electron correlation terms using a more complete numerical model that considers the full three-body Coulomb dynamics. Since an exact quantum treatment is not currently feasible, we resort to a classical trajectory Monte Carlo calculation (CTMC).

In the CTMC simulation, Newton's equations are numerically integrated to track the motion of two spinless electrons. At $t = 0$, e_1 is released from the inner turning point of an $\ell = 2, Z_1 = 1$ continuum orbit. After a delay τ, e_2 is ejected from the inner turning point of an $\ell = 4, Z_2 = 2$ orbit. Typically, a set of ~3000 trajectory pairs is computed for a nominal delay τ. The precise energies of the two electrons and the delay between their respective launch times are varied with each electron pair such that the ensemble distribution reflects the approximate bandwidth and duration of the ionizing laser pulses. The experimental excitation proceeds through the $5dE_1dM = 0$ continuum with $\Delta m_2 = 0$ for the ionization of the $5d$ electron. Therefore, the two electrons are given equal but opposite z components of angular momentum with $-2 \leq m_{1,2} \leq 2$. The relative orbit orientations and launch angles are distributed according to the assumption that all allowed values of m_1 are equally likely. The positions of both electrons are tracked until one of the electrons has a radius $>50\,000$. At this point, recapture has either already occured, will never occur, or has yet to occur but will result in the formation of a Rydberg ion with an effective principal quantum number $n \gg 115$. In the latter case, the Ba^+ ion would be further ionized by the weak clearing pulse in the spectrometer, and therefore would be indistinguishable from an event in which recapture did not occur. At the end of the calculation, electrons with negative total energy are considered to be recaptured. Recapture events are sorted into bins, according to effective principal quantum number, for direct comparison with experiment. Figure 3 shows that in general the agreement between the CTMC simulation results and the experimental data is reasonable.

The classical formalism appears to capture the essential physics of PCI in this system and, therefore, can provide insight into the role of the higher-order terms in V_{ee}. In particular, the simulation predicts that the recaptured electrons do not all have orbital angular momentum $\ell = 2$ (or 4). Instead, a substantial fraction of the ensemble has very high angular momentum; >50% of the bound population is in states with $\ell > 15$. Obviously the $k > 0$ terms play an important role in determining the angular momentum composition of the recaptured wave packet. Yet the success of the shakeup model indicates that those terms do not radically affect the wave packet's energy distribution. Presumably, the wave-mechanical uncertainty in the energy and radial distributions of the two colliding wave packets helps mask higher-order contributions to energy transfer [9]. More importantly though, at large radii, high-n and continuum electrons have kinetic energies and radial trajectories which are nearly independent of $\ell \ll n$. Therefore, we suspect that the sudden approximation provides a good description of the electron dynamics leading to recapture and the net recapture probability, but will not accurately predict the long-term evolution of the resulting bound wave packet.

In summary, we have utilized picosecond laser excitation and wave packet control techniques to provide new insight into a fundamental atomic physics problem. To the best of our knowledge, these are the first explicit time-domain measurements of electron dynamics in a three-body Coulomb continuum. Future experiments may provide more insight into the problem by probing the coherent evolution of the ionic Rydberg wave packet following recapture.

This work has been supported by the NSF and the Packard Foundation.

[1] J. Berakdar and J. S. Briggs, Phys. Rev. Lett. **72**, 3799 (1994).
[2] V. Schmidt *et al.*, Phys. Rev. Lett. **38**, 63 (1977), and references therein.
[3] A. Niehaus, J. Phys. B **10**, 1845 (1977).
[4] A. Niehaus and C. J. Zwakhals, J. Phys. B **16**, L135 (1983).
[5] W. Eberhardt *et al.*, Phys. Rev. A **38**, 3808 (1988).
[6] G. B. Armen *et al.* Phys. Rev. A **36**, 5606 (1987); J. Tulkki *et al.*, Z. Phys. D **5**, 241 (1987).
[7] S. Rioual *et al.*, Phys. Rev. Lett. **86**, 1470 (2001).
[8] T. F. Gallagher, *Rydberg Atoms* (Cambridge University, Cambridge, 1994), 1st ed., and references therein.
[9] Following the launch of e_2, e_1 continues to move. Therefore, the crossing radius R does not actually correspond to the center of the e_1 wave packet at $t = \tau$. However, for large R, the principal quantum number of the recaptured electron increases slowly with crossing radius ($n \sim \sqrt{2R}$). Hence there is little difference between the n values computed at the actual crossing time and at $t = \tau$. This effect, coupled with the uncertainty in R due to the finite radial extent of both wave packets and the fact that states within an energy range ~60 cm^{-1} contribute to each gate, makes the effect of finite e_2 propagation speed negligible.
[10] R. R. Jones and P. H. Bucksbaum, Phys. Rev. Lett. **67**, 3215 (1991); H. Stapelfeldt *et al.*, *ibid.* **67**, 3223 (1991); H. Maeda, W. Li, and T. F. Gallagher, *ibid.* **85**, 5078 (2000).
[11] C. Rosen *et al.*, Phys. Rev. Lett. **83**, 4514 (1999).